MINISTRY OF EDUCATION AND TRAINING

VIETNAM ACADEMY OF SCIENCE AND TECHNOLOGY

GRADUATE UNIVERSITY OF SCIENCE AND TECHNOLOGY

Pham Van Hoan

NONLINEAR STABILITY ANALYSIS OF CYLINDRICAL PANEL AND CYLINDRICAL SHELLS MADE OF FGP MATERIAL SUBJECTED TO MECHANICAL LOADS IN THERMAL ENVIRONMENT

SUMMARY OF DISSERTATION ON MECHANICAL ENGINEERING AND ENGINEERING MECHANICS

Major: Engineering Mechanics

Code: 9520101

Ha Noi - 2024

The dissertation is completed at: Graduate University of Science and Technology, Vietnam Academy of Science and Technology

Supervisors:
Supervisor 1: Assoc, Prof., PhD. Le Kha Hoa
Supervisor 2: Assoc, Prof., PhD. Dao Nhu Mai

Referee 1:.....

Referee 2:.....

Referee 3:.....

The dissertation is examined by Examination Board of Graduate University of Science and Technology, Vietnam Academy of Science and Technology at…….. (time, date……)

The dissertation can be found at:
1. Graduate University of Science and Technology Library
2. National Library of Vietnam

INTRODUCTION

1. The urgency of the thesis

Functionally graded porous (FGP) materials are are designed to have varying porosity and pore structure. By adjusting the distribution and local density of the pores within the material, The mechanical properties of this material can be achieved as desired. FGP materials have been known as a type of lightweight material, exhibit exceptional energyabsorbing capabilities and have found extensive use in various applications.

Cylindrical panel and cylindrical shells serve as fundamental load-bearing elements in contemporary engineering structures. The investigation and analysis of buckling and post-buckling behavior of shell structure made from FGP material have garnered substantial interest among numerous researchers.

From the above analysis, researcher chose the subject: “Nonlinear stability analysis of cylindrical panel and cylindrical shells made of FGP material subjected to mechanical loads in thermal environment”.

2. Objectives of the thesis

Nonlinear stability analysis of cylindrical panel and cylindrical shells made of FGP material subjected to mechanical loads in thermal environment**.**

3. Subject and scope of research of the thesis

The research object of the thesis is cylindrical panel and cylindrical shells are made from functionally graded porous materials (FGP). Research scope of the thesis is shell structures made of FGP materials subject to thermal mechanical loads.

4. Research Methodology

The research method in the thesis is analytical method: Thesis used Donnell shell theory, the first-order shear deformation theory and the improved Lekhnitskii's smeared stiffeners technique in conjunction with the Galerkin method are applied to solve the nonlinear problem.

5. Scientific and practical significance of the thesis

Buckling and post-buckling analysis problems are topics of interest and have important significance in the field of structural mechanics. The

research results provide a scientific basis for designers and manufacturers of FGP structures.

6. Layout of the thesis

The structure of the thesis includes an introduction, four content chapters and a conclusion.

CHAPTER 1. OVERVIEW

Chapter 1 is presented in 16 pages, 10 figures, introducing functionally graded porous (FGP) materials, static stability standards and Research status of nonlinear stability problems of shell structures made from FGM and FGP materials. From there, analyze the issues that have been researched and the issues that need to be further researched in the thesis.

CHAPTER 2. NONLINEAR STABILITY ANALYSIS OF CYLINDRICAL PANEL MADE FROM FGP MATERIAL

Chapter 2 is presented in 31 pages, which include:

2.1. Research problem

Chapter 2 of the thesis uses Donnell shell theory and Galerkin method is applied to solve the following three nonlinear problems

Problem 1: Influence of porosity distribution pattern on the nonlinear stability of porous cylindrical panel under axial compression.

Problem 2: Nonlinear stability of FGP sandwich cylindrical panels with different boundary conditions.

Problem 3: Nonlinear stability of FGP cylindrical sandwich panels on elastic foundation

2.2. Influence of porosity distribution pattern on the nonlinear stability of porous cylindrical panel under axial compression.

Consider a thin circular cylindrical panel and the cylindrical coordinate system with axes *x, y, z* depicted in Figure 2.1.

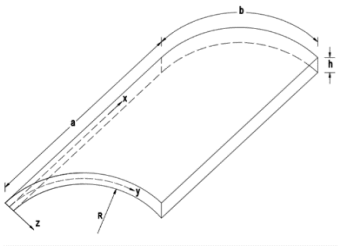

Panel FGP

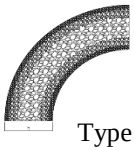

Type a

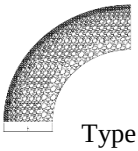

Type b

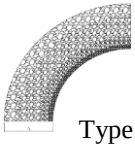

Type c

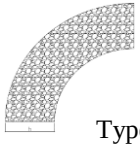

Type d

Figure 2.1: Geometry and coordinate system of a porous circular cylindrical

The porous cylindrical panel is investigated with four porosity distribution types.

Type a: Symmetric porosity distribution

$$E_{sh}(z) = E_{\mathrm{m}}\left[1 - e_0 \cos\left(\frac{\pi z}{h}\right)\right] \tag{2.1a}$$

Type b,c: Non-symmetric porosity distribution

$$E_{sh}(z) = E_{\mathrm{m}}\left[1 - e_0 \cos\left(\frac{\pi z}{2h} + \frac{\pi}{4}\right)\right] \tag{2.1b}$$

$$E_{sh}(z) = E_{\mathrm{m}}\left[1 - e_0 \sin\left(\frac{\pi z}{2h} + \frac{\pi}{4}\right)\right] \tag{2.1c}$$

Type d: uniform porosity distribution

$$E_{sh}(z) = E_{\mathrm{m}}\left(1 - e_0\lambda\right) \tag{2.1d}$$

Based on the Donnell shell theory with von Karman geometrical nonlinearity, the nonlinear equilibrium equations of imperfect FGP cylindrical panel are

$$A_3\nabla^4 f + \frac{1}{R}f_{,xx} + A_4\nabla^4 w + f_{,yy}\left(w_{,xx} + w^*_{,xx}\right) - 2f_{,xy}\left(w_{,xy} + w^*_{,xy}\right) + f_{,xx}\left(w_{,yy} + w^*_{,yy}\right) = 0 \tag{2.18}$$

$$\nabla^4 f + A_1\nabla^4 w - A_2\left(w^2_{,xy} - w_{,xx}w_{,yy} - w_{,xx}/R + 2w_{,xy}w^*_{,xy} - w_{,xx}w^*_{,yy} - w_{,yy}w^*_{,xx}\right) = 0 \tag{2.19}$$

Assume four edges are simply supported

$$\begin{aligned} &w = M_x = N_{xy} = 0,\ N_x = -r_0 h \ \text{ at } \ x = 0,\ x = a \\ &w = M_y = N_{xy} = 0,\ N_y = -p_0 h \ \text{ at } \ y = 0,\ y = b \end{aligned} \tag{2.20}$$

w, *f* function are chosen as

$$w = W\sin\frac{m\pi x}{a}\sin\frac{n\pi y}{b}; \qquad w^* = \xi h\sin\frac{m\pi x}{a}\sin\frac{n\pi y}{b}, \qquad 0 \le \xi \le 1 \tag{2.21}$$
$$f = F\left[\sin\frac{m\pi x}{a}\sin\frac{n\pi y}{b} - \beta(x) - \lambda(y)\right]$$

Substituting equations (2.21) into equation (2.18; 2.19) then using Galerkin method, yields

$$S_1W + S_2W^2 + S_3W\xi h + S_4W(W+\xi h)(W+2\xi h) + \\ +S_5h(W+\xi h)\left(r_0\frac{m^2b^2}{a^2} + p_0n^2\right) - \frac{16b^4}{mn\pi^2}\left(\frac{m^2b^2}{a^2}+n^2\right)^2\frac{p_0h}{R}\delta_1\delta_2 = 0 \tag{2.24}$$

Consider FGP cylindrical panel subjected to axial loading, taking $N_{x0} = -r_0h,\ N_{y0} = -p_0h = 0$, Eq. (2.24) yields

$$r_0 = \frac{a^2}{-S_5m^2hb^2(W+\xi h)}\left[S_1W + S_2W^2 + S_3W\xi h + S_4W(W+\xi h)(W+2\xi h)\right] \tag{2.25}$$

The expression (2.25) is used to determine the critical loads and to analyze the post-buckling load-deflection curves of nonlinear buckling shape of porous cylindrical panel.

Survey results

The effects of porosity distribution pattern are shown in Table 2.3. They show that the critical compression load of the shell made of type a distribution is the biggest, the second is shell made of type b and c distribution, and the critical buckling load of the shell made of type d distribution is the smallest.

Table 2.3. Effects of porosity distribution pattern and e_0 on critical load.

E=2.0779×10^{11} Pa, h=0.01m, b/h=80, a/b = 2, a/R=0.5, ξ=0

r_{cr}(MPa)	e_0=0	e_0=0.3	e_0=0.5	e_0=0.7	e_0=0.9
Type a	393.9363(1,1)	333.8215(1,1)	293.7449 (1,1)	253.6684 (1,1)	212.6000(3,1)
Type b	393.9363(1,1)	319.9092(1,1)	267.5390 (1,1)	210.8125 (1,1)	142.0695(5,1)
Type c	393.9363(1,1)	319.9092(1,1)	267.5390 (1,1)	210.8125 (1,1)	142.0695(5,1)
Type d	393.9363(1,1)	316.2687(1,1)	260.7247 (1,1)	199.7436 (1,1)	125.6195(1,1)

2.3. Nonlinear stability of FGP sandwich cylindrical panels with different boundary conditions

In this study, an symmetric porous sandwich cylindrical panel with FG coating and the cylindrical coordinate system with axes *x*, *y*, *z* as depicted in Figure 2.6.

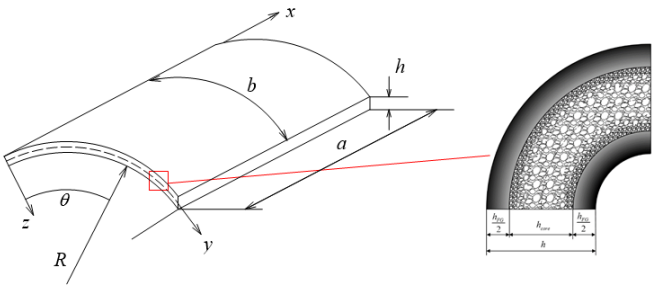

Figure 2.6. Geometry of symmetric porous cylindrical panels with FG coating

Young module and Poisson's ratios of shell is determined

$$\left(E_{sh},\nu_{sh}\right)=\begin{cases}\left(E_c,\nu_c\right)+\left(E_{mc},\nu_{mc}\right)\left(\dfrac{2z+h_{FG}+h_{core}}{h_{FG}}\right)^k, khi\ \dfrac{h_{FG}+h_{core}}{2}\le z\le-\dfrac{h_{core}}{2}\\ \left(E_m,\nu_m\right)\left[1-e_0\cos\left(\dfrac{\pi z}{h_{core}}\right)\right], \text{khi}-\dfrac{h_{core}}{2}\le z\le\dfrac{h_{core}}{2}\\ \left(E_c,\nu_c\right)+\left(E_{mc},\nu_{mc}\right)\left(\dfrac{-2z+h_{FG}+h_{core}}{h_{FG}}\right)^k, \text{khi}\ \dfrac{h_{core}}{2}\le z\le\dfrac{h_{FG}+h_{core}}{2}\end{cases} \tag{2.29}$$

Based on the Donnell shell theory with von Karman geometrical nonlinearity, the nonlinear equilibrium equations of imperfect FGP cylindrical panel are (2.18; 2.19).

Case 1: Four edges are simply supported (SSSS)

Consider FGP cylindrical panel subjected to axial loading, yields is (2.25). Expression (2.25) is established to analyze the stability of an imperfect FGP sandwich cylindrical panel subjected to axial compression.

Case 2: Two edges ($x=0$, $x=a$) are simply supported and two edges are clamped (SSCC).

w, f function are chosen as

$$\begin{aligned}&w=W\sin\frac{m\pi x}{a}\left(1-\cos\frac{2n\pi y}{b}\right)\\ &f=F\left[\sin\frac{m\pi x}{a}\sin\frac{n\pi y}{b}-\lambda(y)\right],\qquad F\frac{d^2\lambda(y)}{dy^2}=r_0h\\ &w^*=\xi h\sin\frac{m\pi x}{a}\left(1-\cos\frac{2n\pi y}{b}\right),\qquad m,n=1,\ 2,\ 3...\end{aligned} \tag{2.31}$$

Substituting Eqs. (2.31) into Eqs. (2.18) and (2.19), and then using Galerkin method, we have

$$r_0 = \frac{-4a}{3bhm^2\pi^2}\left[C_1\frac{W}{(W+\xi h)} + C_2\frac{W(W+2\xi h)}{(W+\xi h)} + C_3 W + C_4 W(W+2\xi h)\right] \quad (2.34)$$

The expression (2.34) is used to nonlinear stability of FGP sandwich cylindrical panels with different boundary conditions

Survey results

Table 2.6. Influence of e_0 and core layer h_{core}/h_{FG} on critical load. p=1, h=0.006m, a/b=1.5, b/h=50, a/R=0.5, ξ=0.

r_{cr} (MN)	Boundary conditions	e_0=0	e_0=0.5	e_0=0.8
h_{core}/h_{FG}=0	SSSS	587.0261(1,1)	587.0261 (1,1)	587.0261 (1,1)
	SSCC	677.8399 (3,1)	677.8399 (3,1)	677.8399 (3,1)
h_{core}/h_{FG}=5	SSSS	468.9710 (1,1)	382.9550 (1,1)	331.3454 (1,1)
	SSCC	537.8872 (3,1)	457.3689 (3,1)	409.0579 (3,1)
h_{core}/h_{FG}=10	SSSS	452.4019 (3,1)	355.5114 (1,1)	296.8736 (1,1)
	SSCC	516.6474(3,1)	422.1734(3,1)	365.4889(3,1)

Table 2.6 shows that the critical axial load decreases when porosity coefficients e_0 or h_{core}/h_{FG} increases. The effects of two types boundary conditions on buckling and post-buckling behavior of porous sandwich cylindrical panels have been also carried out. It can be seen that the critical axial loads when panels are simply supported four edges, are smaller than ones when those structures are simply supported two edges and clamped two edges.

Figure 2.10 shows when value of volume fraction index increases, the critical buckling load increases.

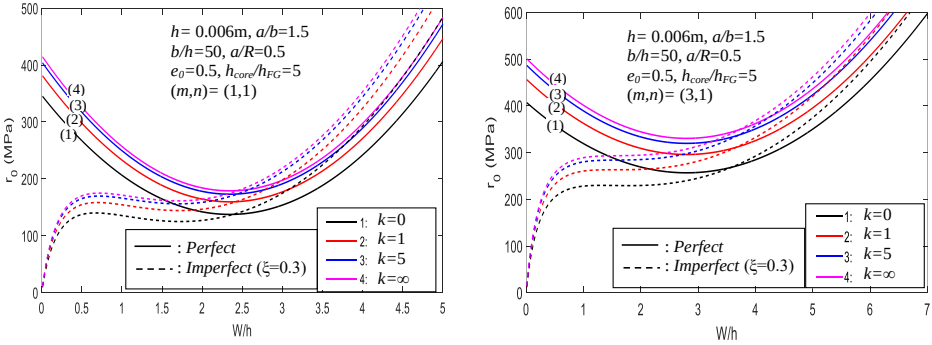

(a) FGP cylindrical panels with SSSS (b) FGP cylindrical panels with SSCC

Figure 2.10. Influence of p on $r_0 - W/h$ paths

2.4. Nonlinear stability of FGP cylindrical sandwich panels on elastic foundation

In this study, an symmetric porous sandwich cylindrical panel with FG coating and the cylindrical coordinate system with axes *x, y, z* as depicted in Figure 2.6.

Young moduli and Poisson's ratios of shell is determined (2.29).

Based on the Donnell shell theory with von Karman geometrical nonlinearity, the nonlinear equilibrium equations of imperfect FGP cylindrical panel, taking into account a two-parameter elastic foundation are (2.19) and (2.38)

$$\begin{aligned} &A_3\nabla^4 f + \frac{1}{R} f_{,xx} + A_4\nabla^4 w + f_{,yy}\left(w_{,xx} + w^*_{,xx}\right) - 2f_{,xy}\left(w_{,xy} + w^*_{,xy}\right) + \\ &+ f_{,xx}\left(w_{,yy} + w^*_{,yy}\right) + K_2(w_{,xx} + w_{,yy}) - K_1 w = 0 \end{aligned} \tag{2.38}$$

Assume four edges are simply supported. the *w* function are chosen as

$$w = W\sin\frac{m\pi}{a}x\sin\frac{n\pi}{b}y; \quad w^* = \xi h\sin\frac{m\pi}{a}x\sin\frac{n\pi}{b}y, \ m, n = 1, 2, 3.... \tag{2.39}$$

Substituting equations (2.39 into equation (2.19; 2.38) then using Galerkin method, yields

$$\begin{aligned} &S_1^*W + S_2^*(W^2 + 2\xi hW) + S_3^*W(\xi h + W) - S_4^*(\xi h + W)(W^2 + 2\xi hW) \\ &-\frac{1}{4}\left[K_2\left(\frac{m^2\pi^2}{a^2} + \frac{n^2\pi^2}{b^2}\right) + K_1\right]W = (\xi h + W)\frac{1}{4}\left(N_x\frac{m^2\pi^2}{a^2} + N_y\frac{n^2\pi^2}{b^2}\right) - \frac{N_y}{R}\frac{4}{mn\pi^2}\delta_1\delta_2 \end{aligned} \tag{2.41}$$

Consider FGP cylindrical panel subjected to axial loading, taking $N_{x0} = -r_0 h,\ N_{y0} = -p_0 h = 0$, Eq. (2.41) yields

$$r_0 = \frac{-4a^2}{hm^2\pi^2(\xi h + W)}\left\{\begin{aligned} &S_1W + S_2W(W + 2\xi h) + S_3W(\xi h + W) \\ &-S_4W(\xi h + W)(W + 2\xi h) - \frac{1}{4}\left[K_2\left(\frac{m^2\pi^2}{a^2} + \frac{n^2\pi^2}{b^2}\right) + K_1\right]W \end{aligned}\right\} \tag{2.42}$$

The expression (2.42) is used to nonlinear stability of FGP cylindrical sandwich panels on elastic foundation.

Survey results

Looking at Figure 2.17, it can see that the upper axial load increase when the foundation coefficients increases.

Figure 2.20 shows the postbuckling load-deflection curves of perfect and imperfect porous panels. It can be seen that, the curves of imperfect porous panels start at original coordinates and the curves of perfect porous

panels start at a point on the vertical axis of coordinates that means the deflection of the perfect porous panels only appears when the axial compression load is large enough – buckling load.

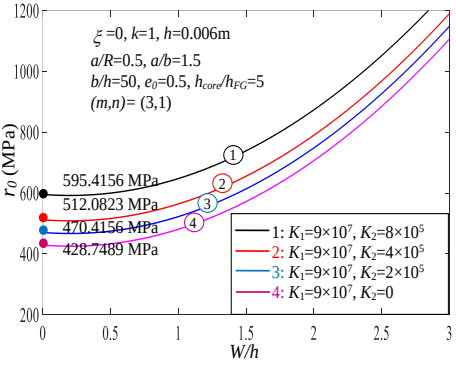

Figure 2.17. Influence of K_1 and K_2 on $r_0 - W/h$

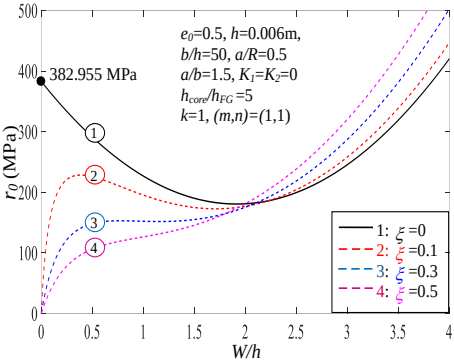

Figure 2.20. Influence of ξ on $r_0 - W/h$

Conclusion of Chapter 2

The content of Chapter 2 of the thesis addresses the following issues

1. Analyzed influence of porosity distribution pattern on the nonlinear stability of porous cylindrical panel under axial compression.

2. Analyzed nonlinear stability of FGP sandwich cylindrical panels with different boundary conditions.

3. Analyzed nonlinear stability of FGP cylindrical sandwich panels on elastic foundation

CHAPTER 3. NONLINEAR STABILITY OF ES-FG POROUS SANDWICH CYLINDRICAL SHELLS SUBJECTED TO AXIAL COMPRESSION OR EXTERNAL PRESSURE

Chapter 3 is presented in 37 pages, which include:

3.1. Research problem

Chapter 3 of the thesis uses Donnell shell theory, the improved Lekhnitskii's smeared stiffeners technique, Galerkin method is applied to solve the following three nonlinear problems

Problem 1: Influence of porosity distribution pattern on the nonlinear stability of porous cylindrical shells under axial compression

Problem 2: Nonlinear stability of ES-FG porous sandwich cylindrical shells subjected to axial compression

Problem 3: Nonlinear stability of ES-FG porous sandwich cylindrical shells under external pressure

3.2. Influence of porosity distribution pattern on the nonlinear stability of porous cylindrical shells under axial compression

Consider a thin circular cylindrical shell with mean radius *R*, thickness *h* and length *L* only subjected to uniform axial compression load with intensity *p* surrounded by elastic foundation in thermal environment. The middle surface of the shells is referred to the coordinates x, y, z as shown in Figure 3.1. The porous cylindrical shell is investigated in this work with four porosity distribution types which are depicted in Figure 3.2.

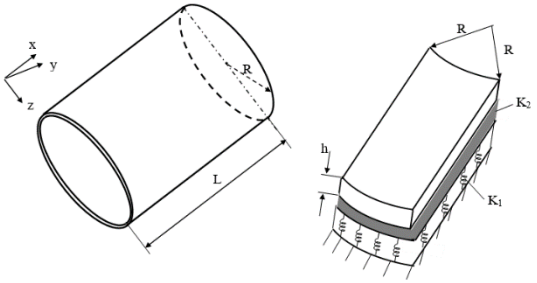

Figure 3.1. Geometry and coordinate system of a porous circular cylindrical shell surrounded by elastic foundation.

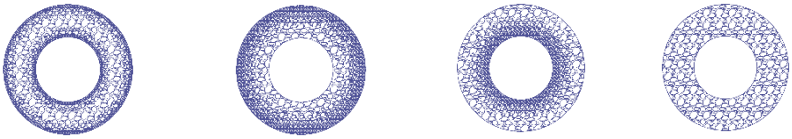

Type 1 Type 2a Type 2b Type 3

Figure 3.2. Cross-section of a FGP cylindrical shell with different porosity distributions

Young's modulus and coefficient of thermal expansion of the porous cylindrical shells

Type 1: Symmetric porosity distribution

$$E_{sh}(z) = E_{\mathrm{m}}\left[1 - e_0 \cos\left(\frac{\pi z}{h}\right)\right]; \quad \alpha_{sh}(z) = \alpha_{\mathrm{m}}\left[1 - e_0 \cos\left(\frac{\pi z}{h}\right)\right] \qquad (3.1)$$

Type 2a,b: Non-symmetric porosity distribution

$$E_{sh}(z) = E_{\mathrm{m}}\left[1 - e_0 \cos\left(\frac{\pi z}{2h} + \frac{\pi}{4}\right)\right]; \quad \alpha_{sh}(z) = \alpha_{\mathrm{m}}\left[1 - e_0 \cos\left(\frac{\pi z}{2h} + \frac{\pi}{4}\right)\right] \tag{3.2a}$$

$$E_{sh}(z) = E_{\mathrm{m}}\left[1 - e_0 \sin\left(\frac{\pi z}{2h} + \frac{\pi}{4}\right)\right]; \quad \alpha_{sh}(z) = \alpha_{\mathrm{m}}\left[1 - e_0 \sin\left(\frac{\pi z}{2h} + \frac{\pi}{4}\right)\right] \tag{3.2b}$$

Type 3: uniform porosity distribution

$$E_{sh}(z) = E_{\mathrm{m}}\left(1 - e_0\lambda\right); \quad \alpha_{sh}(z) = \alpha_{\mathrm{m}}\left(1 - e_0\lambda\right) \tag{3.3}$$

Based on the Donnell shell theory with von Karman geometrical nonlinearity, the nonlinear governing equations of porous cylindrical shells in thermal environment, taking into account an elastic foundation are

$$A_3\nabla^4\varphi + \frac{1}{R}\varphi_{,xx} + A_4\nabla^4 w + \varphi_{,yy}w_{,xx} - 2\varphi_{,xy}w_{,xy} + K_2\left(w_{,xx} + w_{,yy}\right) - K_1 w = 0 \tag{3.4}$$

$$\nabla^4\varphi + A_1\nabla^4 w - A_2\left(w_{,xy}^2 - w_{,xx}w_{,yy} - w_{,xx}/R\right) = 0 \tag{3.5}$$

Assuming that the cylindrical shell is simply supported at the edges $x = 0$ and $x = L$. The deflection of axially loaded shell

$$w = w(x, y) = f_0 + f_1 \sin\alpha x.\sin\beta y + f_2 \sin^2\alpha x \tag{3.6}$$

Substituting Eq. (3.6) into Eq. (3.4; 3.5), then applying Galerkin method in the ranges $0 \le y \le 2\pi R$ and $0 \le x \le L$, lead to

$$-\frac{2\sigma_{0y}h}{R} - K_1\left(f_2 + 2f_0\right) = 0 \tag{3.9}$$

$$f_1^2 = \frac{ph\alpha^2 + \sigma_{0y}h.\beta^2 - \left[H_{01} + H_{04}f_2^2 + H_{05}f_2 + K_2\left(\alpha^2 + \beta^2\right) + K_1\right]}{H_{03}} \tag{3.10}$$

$$H_{06}f_2 + 8\alpha^2 f_2 ph + H_{07}f_1^2 + H_{08}f_1^2 f_2 - 8\frac{\sigma_{0y}h}{R} - 8K_2\alpha^2 f_2 - 6K_1 f_2 - 8K_1 f_0 = 0 \tag{3.11}$$

The circumferentially closed condition of cylinder, lead to

$$8C_{12}^* ph - 8\frac{1}{A_2}\sigma_{0y}h + \frac{4}{R}\left(2f_0 + f_2\right) - \beta^2 f_1^2 + 8C_{26}^*\phi_1 = 0 \tag{3.12}$$

Using equations (3.9-3.12), lead to

$$p = -\frac{1}{\left[H_{07}L_{11} + \left(8\alpha^2 + H_{08}L_{11}\right)f_2\right]h}\left[H_{07}L_{12} + \left(H_{06} + H_{07}L_{13} + H_{08}L_{12} - 8K_2\alpha^2 - 4K_1\right)f_2\right.$$
$$\left. + \left(H_{07}L_{14} + H_{08}L_{13}\right)f_2^2 + H_{08}L_{14}f_2^3 - 8RK_1\beta^2 L_0\left(\frac{H_{07}}{H_{03}} + \frac{H_{08}}{H_{03}}f_2\right)C_{26}^*\phi_1\right] \tag{3.17}$$

That the maximal deflection of shells

$$W_{\max} = L_{01}ph + L_{02} + (L_{03}+1) f_2 + L_{04} f_2^2 + 8L_0 C_{26}^* \phi_1 + \left[L_{11}ph + L_{12} + L_{13} f_2 + L_{14} f_2^2 - \frac{8RK_1\beta^2 L_0}{H_{03}} C_{26}^* \phi_1 \right]^{1/2} \quad (3.20)$$

Combining equations (3.17) with (3.20), the effects of porosity distribution pattern, foundation parameters, and temperature on the post-buckling load - maximal deflection curves of porous cylindrical shells can be analyzed.

Survey results

Table 3.3. Effects of porosity distribution pattern and ΔT on critical load for porous cylindrical shells. h=0.01m, R/h=100, L/R=1.5, e_0=0.4 , K_1=2×10^{7}N/m^3, K_2=1.5×10^{5}N/m

p_{cr} (MPa)	ΔT=0K	ΔT=200K	ΔT=400K	ΔT=600K	ΔT=800K
Type 1	1026.9885 (8,4)	984.9455 (8,4)	892.0460 (8,4)	748.2919 (8,4)	553.3334 (6,8)
Type 2a	1884.2215 (12,2)	1806.6467 (12,2)	1634.6992 (12,2)	1368.3791 (12,2)	1007.6865 (12,2)
Type 2b	962.2595 (8,5)	922.7552 (8,5)	835.6489 (8,5)	700.9435 (8,5)	518.5824 (7,7)
Type 3	945.7243 (8,5)	906.9270 (8,5)	821.3684 (8,5)	689.0515 (8,5)	509.9844 (8,5)

The effects of porosity distribution pattern are shown in Table 3.3. They show that the critical compression load of the shell made of type 2a distribution is the biggest, the second is shell made of type 1 distribution, and the third is with made of type 2b distribution. The critical buckling load of the shell made of type 3 distribution is the smallest. Table 3 also show that the critical load of shell reduces when ΔT increases.

3.3. Nonlinear stability of ES-FG porous sandwich cylindrical shells subjected to axial compression

Let's examine an eccentrically stiffened - functionally graded porous sandwich cylindrical shell under uniform axial compression (load intensity denoted as p) on an elastic foundation within thermal environment, as depicted in Figure 3.7.

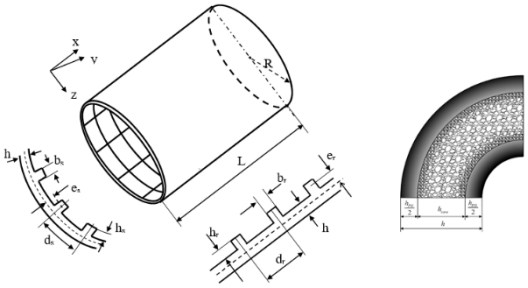

Figure 3.7. The structural and coordinate system of a stiffened FG porous sandwich cylindrical shell

Young module and thermal expansion of three-layered shell

$$\begin{pmatrix} E_{sh} \\ \alpha_{sh} \end{pmatrix} = \begin{cases} \begin{pmatrix} E_c \\ \alpha_c \end{pmatrix} + \begin{pmatrix} E_{mc} \\ \alpha_{mc} \end{pmatrix} \left(\dfrac{2z + h_{FG} + h_{core}}{h_{FG}} \right)^k, & -\dfrac{h_{FG} + h_{core}}{2} \le z \le -\dfrac{h_{core}}{2} \\ \begin{pmatrix} E_m \\ \alpha_m \end{pmatrix} \left[1 - e_0 \cos\left(\dfrac{\pi z}{h_{core}} \right) \right], & -\dfrac{h_{core}}{2} \le z \le \dfrac{h_{core}}{2} \\ \begin{pmatrix} E_c \\ \alpha_c \end{pmatrix} + \begin{pmatrix} E_{mc} \\ \alpha_{mc} \end{pmatrix} \left(\dfrac{-2z + h_{FG} + h_{core}}{h_{FG}} \right)^k, & \dfrac{h_{core}}{2} \le z \le \dfrac{h_{FG} + h_{core}}{2} \end{cases} \tag{3.21}$$

Incase 1: Inside stiffened cylindrical shell

$$\begin{cases} \begin{pmatrix} E_s \\ \alpha_s \end{pmatrix} = \begin{pmatrix} E_c \\ \alpha_c \end{pmatrix} + \begin{pmatrix} E_{mc} \\ \alpha_{mc} \end{pmatrix} \left(\dfrac{2z - h}{2h_s} \right)^{k_2}, & \dfrac{h}{2} \le z \le \dfrac{h}{2} + h_s \\ \begin{pmatrix} E_r \\ \alpha_r \end{pmatrix} = \begin{pmatrix} E_c \\ \alpha_c \end{pmatrix} + \begin{pmatrix} E_{mc} \\ \alpha_{mc} \end{pmatrix} \left(\dfrac{2z - h}{2h_r} \right)^{k_3}, & \dfrac{h}{2} \le z \le \dfrac{h}{2} + h_r \end{cases} \tag{3.22}$$

Incase 2: Inside stiffened cylindrical shell

$$\begin{cases} \begin{pmatrix} E_s \\ \alpha_s \end{pmatrix} = \begin{pmatrix} E_c \\ \alpha_c \end{pmatrix} + \begin{pmatrix} E_{mc} \\ \alpha_{mc} \end{pmatrix} \left(-\dfrac{2z + h}{2h_s} \right)^{k_2} & -\dfrac{h}{2} - h_s \le z \le -\dfrac{h}{2} \\ \begin{pmatrix} E_r \\ \alpha_r \end{pmatrix} = \begin{pmatrix} E_c \\ \alpha_c \end{pmatrix} + \begin{pmatrix} E_{mc} \\ \alpha_{mc} \end{pmatrix} \left(-\dfrac{2z + h}{2h_r} \right)^{k_3} & -\dfrac{h}{2} - h_r \le z \le -\dfrac{h}{2} \end{cases} \tag{3.23}$$

Based on the Donnell shell theory with von Karman geometrical nonlinearity, the nonlinear governing equations of ES-FG porous cylindrical shells in thermal environment, taking into account an elastic foundation are

$$\begin{aligned} &\alpha_{11} w_{,xxxx} + \alpha_{12} w_{,xxyy} + \alpha_{13} w_{,yyyy} + \alpha_{14} \varphi_{,xxxx} + \alpha_{15} \varphi_{,xxyy} + \alpha_{16} \varphi_{,yyyy} \\ &+ \frac{1}{R} \varphi_{,xx} + \varphi_{,yy} w_{,xx} + \varphi_{,xx} w_{,yy} - 2\varphi_{,xy} w_{,xy} + K_2 \left(w_{,xx} + w_{,yy} \right) - K_1 w = 0 \end{aligned} \tag{3.35}$$

$$\beta_{11}\varphi_{,xxxx}+\beta_{12}\varphi_{,xxyy}+\beta_{13}\varphi_{,yyyy}+\beta_{14}w_{,xxxx}+\beta_{15}w_{,xxyy}+\beta_{16}w_{,yyyy}-w_{,xy}^{2}+w_{,xx}w_{,yy}+\frac{1}{R}w_{,xx}=0 \quad (3.36)$$

Assuming that the boundary conditions at two edges $x=0$ and $x=L$ of cylinder is simply supported. The deflection of shell under axial load is (3.6) Substituting Eq. (3.6) into Eq. (3.35; 3.36), then applying Galerkin procedure, result in

$$\sigma_{0y}=-\frac{RK_1\left(f_2+2f_0\right)}{2h} \quad (3.38)$$

$$f_1^2=\frac{ph\alpha^2+\sigma_{0y}h.\beta^2-\left[H_{01}+H_{04}f_2^2+H_{05}f_2+K_2\left(\alpha^2+\beta^2\right)+K_1\right]}{H_{03}} \quad (3.39)$$

$$H_{06}f_2+8\alpha^2f_2ph+H_{07}f_1^2+H_{08}f_1^2f_2-8\frac{\sigma_{0y}h}{R}-8K_2\alpha^2f_2-6K_1f_2-8K_1f_0=0 \quad (3.40)$$

The circumferentially closed condition of cylinder, lead to

$$8C_{12}^{*}ph-8C_{11}^{*}\sigma_{0y}h+\frac{4}{R}\left(2f_0+f_2\right)-\beta^2f_1^2+8\left(C_{26}^{*}\phi_1-C_{12}^{*}\phi_{1x}^{T}+C_{11}^{*}\phi_{1y}^{T}\right)=0 \quad (3.41)$$

Using equations (3.38-3.41), lead to

$$\begin{aligned}p=&-\frac{1}{\left[H_{07}L_{11}+\left(8\alpha^2+H_{08}L_{11}\right)f_2\right]h}\left[H_{07}L_{12}\right.\\&+\left(H_{06}+H_{07}L_{13}+H_{08}L_{12}-8K_2\alpha^2-4K_1\right)f_2+\left(H_{07}L_{14}+H_{08}L_{13}\right)f_2^2\\&\left.+H_{08}L_{14}f_2^3-8RK_1\beta^2L_0\left(\frac{H_{07}}{H_{03}}+\frac{H_{08}}{H_{03}}f_2\right)\left(C_{26}^{*}\phi_1-C_{12}^{*}\phi_{1x}^{T}+C_{11}^{*}\phi_{1y}^{T}\right)\right]\end{aligned} \quad (3.46)$$

The upper buckling compressive load

$$p_{upper}=-\frac{1}{H_{03}L_{11}h}\left[H_{03}L_{12}-8RK_1\beta^2L_0\left(C_{26}^{*}\phi_1-C_{12}^{*}\phi_{1x}^{T}+C_{11}^{*}\phi_{1y}^{T}\right)\right] \quad (3.47)$$

That the maximal deflection of shells

$$\begin{aligned}W_{\max}=&L_{01}ph+L_{02}+\left(L_{03}+1\right)f_2+L_{04}f_2^2+8L_0\left(C_{26}^{*}\phi_1-C_{12}^{*}\phi_{1x}^{T}+C_{11}^{*}\phi_{1y}^{T}\right)\\&+\left[L_{11}ph+L_{12}+L_{13}f_2+L_{14}f_2^2-\frac{8RK_1\beta^2L_0}{H_{03}}\left(C_{26}^{*}\phi_1-C_{12}^{*}\phi_{1x}^{T}+C_{11}^{*}\phi_{1y}^{T}\right)\right]^{1/2}\end{aligned} \quad (3.48)$$

By merging Eq. (3.46) and Eq. (3.48), it becomes possible to scrutinize the impact of material and geometric factors on the post-buckling load-maximum deflection curves of shells.

Incase $f_1=0$ and $f_2=0$, the average end-shortening ratio $\overline{\Delta}_x$ as

$$\overline{\Delta}_x = \left[C^*_{22} - \frac{C^{*2}_{12} R^2 K_1}{C^*_{11} K_1 R^2 + 1} \right] ph - \frac{C^*_{12} R^2 K_1}{C^*_{11} K_1 R^2 + 1} \left(C^*_{26} \phi_1 - C^*_{12} \phi^T_{1x} + C^*_{11} \phi^T_{1y} \right) - \left(C^*_{16} \phi_1 + C^*_{22} \phi^T_{1x} - C^*_{12} \phi^T_{1y} \right) \quad (3.53)$$

Combining Eq. (3.46) with Eqs. (3.53), The analysis can explore how inhomogeneous and dimensional parameters affect the curves depicting post-buckling loads and average end-shortening ratios of shells.

Survey results

Figure 3.11 illustrates the impact of ΔT on p - $\overline{\Delta}_x$ postbuckling curves. As observed, the starting point of lines with $\Delta T \neq 0K$ is not on the vertical axis of the coordinates. This implies that the temperature field causes the shell to deflect outward (resulting in negative deflection) before the mechanical load is applied. When the shell experiences an axial load, its outward deflection diminishes. Upon surpassing the bifurcation point of the load, an inward deflection is observed. As ΔT increases, both the upper and lower axial loads of the shell decrease.

Observing Figs 3.12, it's evident that as the porosity coefficients e_0 increase, the curves demonstrate a lower trajectory.

The influence of k and the foundation on the bearing capacity of shells is depicted in Figs. 3.16 and 3.17. The research reveals that the critical buckling load diminishes as k decreases. And when the foundation parameters K_1 and K_2 increase, the critical load value also increases. Specifically, the shell's critical load is smallest when there is no foundation.

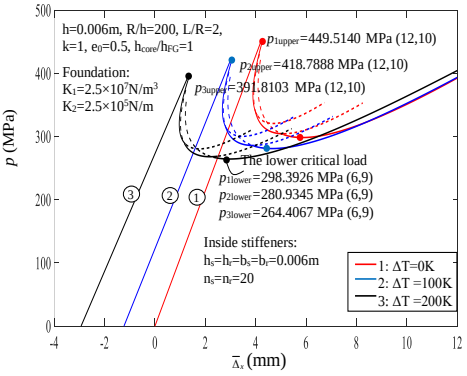

Figure 3.11. The impact of ΔT on p - $\overline{\Delta}_x$ curves

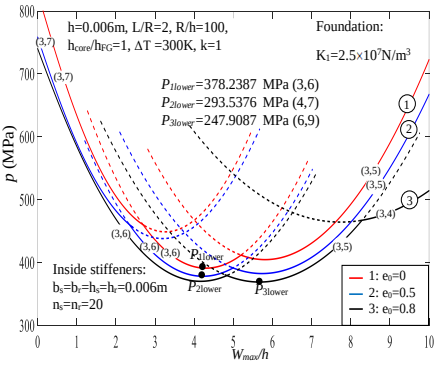

Figure 3.12. The impact of e_0 on p - W_{max}/h curves

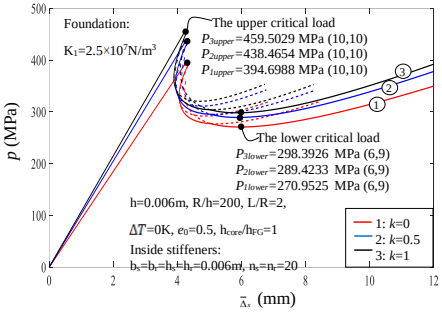

Figure 3.16. The impact of k on p - $\bar{\Delta}_x$ curves

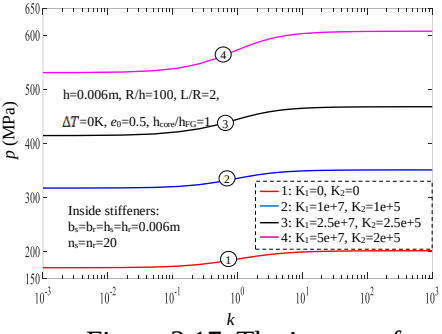

Figure 3.17. The impact of foundation on

Table 3.12. The impact of stiffener on critical load for ES-FG porous sandwich cylinders. k=1; ΔT=300^{0}C; h=0.006m; L/R=2; b_s=b_r=0.006m; h_s=h_r=0.006m; K_1=2.5×10^{7}N/m^3; K_2=2.5×10^{5}N/m; e_0 =0.5; h_{core}/h_{FG}=1

p_{cr} (MPa)		R/h=100	R/h=200	R/h=300
Không gân (n_s= n_r=0)		630.2644 (11,1)*	343.7590 (16,1)	250.9132 (19,5)
n_s=40, n_r=0	Gân trong	708.2389 (5,8)	378.9682 (10,12)	263.3646 (13,15)
	Gân ngoài	745.4105 (6,8)	381.2173 (13,8)	266.0357 (14,14)
n_s=20, n_r=20	Gân trong	698.5920 (7,8)	367.6248 (12,10)	258.7624 (14,14)
	Gân ngoài	749.6283 (10,2)	373.9650 (15,1)	264.8245 (19,3)
n_s=0, n_r=40	Gân trong	644.5673 (9,7)	350.7274 (13,9)	251.3729 (16,13)
	Gân ngoài	703.1807 (12,1)	361.1648 (16,1)	258.5777 (20,1)

Table 3.12 demonstrates the impact of stiffeners on both the upper and lower critical loads of ES-FG porous sandwich cylindrical shells. It is evident that both the upper and lower critical axial loads of ES-FG porous sandwich cylinders reinforced by outside stiffeners is bigger than inside stiffeners and the worst bearing capacity is the unreinforced shell. Furthermore, Table 7 indicates that among shells with identical numbers of stiffeners, the critical axial load is highest for the shell reinforced by rings, followed by the shell reinforced by orthogonal stiffeners, with the shell reinforced by stringers being third. The unstiffened shell exhibits the lowest critical buckling load.

3.4. Nonlinear stability of ES-FG porous sandwich cylindrical shells under external pressure

Consider an eccentrically stiffened FG-porous cylinder subjected to external pressure as shown in figure 3.7.

Young's moduli of shell and inside FGM stiffener are expressed by (3.21) and (3.22).

Based on the Donnell shell theory with von Karman geometrical nonlinearity and smeared stiffeners technique, the governing equations are (3.56) and (3.36)

$$\begin{aligned}&\alpha_{11}w_{,xxxx}+\alpha_{12}w_{,xxyy}+\alpha_{13}w_{,yyyy}+\alpha_{14}\varphi_{,xxxx}+\alpha_{15}\varphi_{,xxyy}+\alpha_{16}\varphi_{,yyyy}\\&+\varphi_{,xx}/R+\varphi_{,xx}w_{,yy}+\varphi_{,yy}w_{,xx}-2\varphi_{,xy}w_{,xy}+K_2\left(w_{,xx}+w_{,yy}\right)-K_1w+q=0\end{aligned}\tag{3.56}$$

Assuming that the boundary conditions at two edges $x=0$ and $x=L$ of cylinder is simply supported. The deflection of shell under axial load is (3.6)

External pressure is

$$q=-\frac{1}{\left(D_{07}L_{A11}+D_{08}L_{A11}f_2\right)}\times\begin{bmatrix}D_{07}L_{A12}+\left(D_{06}+D_{07}L_{A13}+L_{A12}D_{08}-8K_2\alpha^2-2K_1\right)f_2\\+\left(D_{07}L_{A14}+L_{A13}D_{08}\right)f_2^2+L_{A14}D_{08}f_2^3\end{bmatrix}\tag{3.64}$$

Expression (3.64) is used to determine the buckling loads and to analyze the postbuckling response.

Maximal deflection of the shells is

$$W_{\max}=L_{A01}q+L_{A02}+\left(L_{A03}+1\right)f_2+L_{A04}f_2^2+\left(L_{A11}q+L_{A12}+L_{A13}f_2+L_{A14}f_2^2\right)^{1/2}\tag{3.66}$$

Combining Eq. (3.64) with Eq. (3.66), the effects of the geometric parameter, porosity parameters, the thickness of the porous core, stiffeners, foundation, and material parameters on the post-buckling load - maximal deflection curves of cylinder can be analyzed.

Survey results

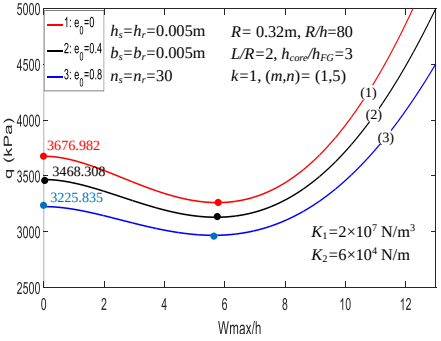

Figure 3.20. Effects of porosity cofficient e_0 on q–W_{max}/h curves

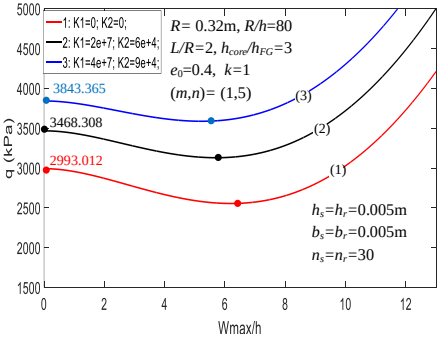

Figure 3.21. Effects of foundation on q–W_{max}/h curves

Fig. 3.20 indicates that the load-carrying of the sandwich cylinder is decreased when e_0 is increased. Fig. 3.21, observed that the critical external pressure increase when the foundation parameters K_1 and K_2 separately or together increase.

Table 3.16. Effects of stiffeners and volume fraction index on critical pressure. h=4mm, R/h=80, L/R=2, h_{core}/h_{FG}=3, h_s=5mm, h_r=5mm, b_s=5mm, b_r=5mm, n_s=30, n_r=30, ΔT=0K, $K_1=2\times10^7$ N/m^3 $K_2=6\times10^4$ N/m, e_0=0.4

q_{cr} (kPa)	Unstiffened	Stringer (n_s=60)	Ring (n_r=60)	Orthogonal (n_s=n_r=30)
k=0	1237.277 (1,6)	1244.460 (1,6)	4687.754 (1,4)	3761.575 (1,5)
k=1	1393.725 (1,6)	1400.241 (1,6)	4516.512 (1,4)	3468.308 (1,5)
k=5	1485.786 (1,6)	1491.131 (1,6)	4534.340 (1,4)	3407.016 (1,5)
k=∞	1524.934 (1,6)	1529.547 (1,6)	4552.000 (1,4)	3385.620 (1,5)

Table 3.16, the critical load of un-stiffened FGM shell is the smallest, the critical load of FGP cylindrical shell reinforced by rings is biggest.

Conclusion of Chapter 3

The content of Chapter 3 of the thesis addresses the following issues

1. Analyzed influence of porosity distribution pattern on the nonlinear stability of porous cylindrical panel under axial compression.

2. Analyzed nonlinear stability of FGP sandwich cylindrical panels with different boundary conditions.

3. Analyzed nonlinear stability of FGP cylindrical sandwich panels on elastic foundation

CHAPTER 4. NONLINEAR STABILITY ANALYSIS OF A CYLINDRICAL SANDWICH FGP UNDER TORSIONAL LOAD

Chapter 4 is presented in 30 pages, which include:

4.1. Research problem

Chapter 4 of the thesis uses Donnell shell theory, the first order shear deformation theory, the improved Lekhnitskii's smeared stiffeners technique, Galerkin method is applied to solve the following three nonlinear problems

Problem 1: Nonlinear behavior of FG porous cylindrical sandwich shells reinforced by spiral stiffeners under torsional load

Problem 2: Nonlinear stability of ES-FG porous sandwich cylindrical

shells subjected to torsional load

4.2. Nonlinear behavior of FG porous cylindrical sandwich shells reinforced by spiral stiffeners under torsional load

In this study, a spiral stiffened FGP cylinder with two FG coating under torsion load as shown in Fig. 4.1 is considered.

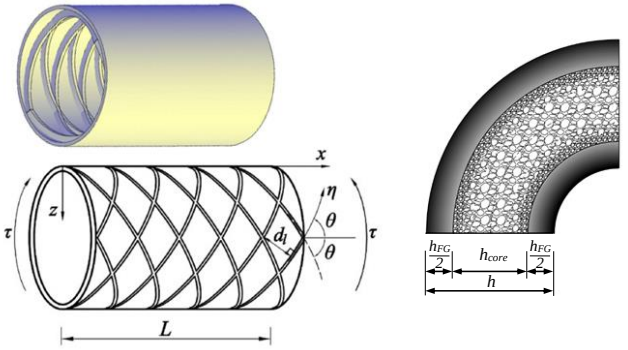

Figure 4.1. Spiral stiffened FGP sandwich cylinder

$$\cos\theta = \left(n_p d_p\right)/\left(2\pi R\right)$$

Young module and thermal expansion of three-layered shell

$$\begin{pmatrix} E_{sh} \\ \alpha_{sh} \end{pmatrix} = \begin{cases} \begin{pmatrix} E_c \\ \alpha_c \end{pmatrix} + \begin{pmatrix} E_{mc} \\ \alpha_{mc} \end{pmatrix}\left(\frac{2z + h_{FG} + h_{core}}{h_{FG}}\right)^k & -\frac{h_{FG}+h_{core}}{2} < z < -\frac{h_{core}}{2} \\ \begin{pmatrix} E_m \\ \alpha_m \end{pmatrix}\left[1 - e_0 \cos\left(\frac{\pi z}{h_{core}}\right)\right] & -\frac{h_{core}}{2} < z < \frac{h_{core}}{2} \\ \begin{pmatrix} E_c \\ \alpha_c \end{pmatrix} + \begin{pmatrix} E_{mc} \\ \alpha_{mc} \end{pmatrix}\left(\frac{-2z + h_{FG} + h_{core}}{h_{FG}}\right)^k & \frac{h_{core}}{2} < z < \frac{h_{FG}+h_{core}}{2} \end{cases} \quad (3.21)$$

Inside spiral stiffener

$$\begin{pmatrix} E_p \\ \alpha_p \end{pmatrix} = \begin{pmatrix} E_c \\ \alpha_c \end{pmatrix} + \begin{pmatrix} E_{mc} \\ \alpha_{mc} \end{pmatrix}\left(\frac{2z-h}{2h_p}\right)^{k_p} \quad (4.1)$$

Based on the Donnell shell theory with von Karman geometrical nonlinearity, the nonlinear governing equations of FGP porous cylindrical shells under torsional load, in thermal environment taking into account an elastic foundation are

$$\alpha_{11}w_{,xxxx}+\alpha_{12}w_{,xxyy}+\alpha_{13}w_{,yyyy}+\alpha_{14}A_{,xxxx}+\alpha_{15}A_{,xxyy}+\alpha_{16}A_{,yyyy}$$
$$+\frac{1}{R}A_{,xx}+A_{,yy}w_{,xx}+A_{,xx}w_{,yy}-2A_{,xy}w_{,xy}-K_1w+K_2\left(w_{,xx}+w_{,yy}\right)=0 \tag{4.10}$$

$$\beta_{11}A_{,xxxx}+\beta_{12}A_{,xxyy}+\beta_{13}A_{,yyyy}+\beta_{14}w_{,xxxx}+\beta_{15}w_{,xxyy}+\beta_{16}w_{,yyyy}-\left(w_{,xy}\right)^2+$$
$$+w_{,xx}.w_{,yy}+\frac{w_{,xx}}{R}=0 \tag{4.11}$$

Consider the simply supported cylindrical shell at two butt-ends $x=0$ and $x=L$, the deflection of the shell is assumed as

$$w=w(x,y)=f_0+f_1\sin\alpha x\sin\beta\left(y-\lambda x\right)+f_2\sin^2\alpha x \tag{4.12}$$

Applying Galerkin procedure, result in

$$\left[2\tau h\beta^2\lambda+D_1+D_2f_2+D_3f_1^2+D_4f_2^2-K_1-K_2\left(\alpha^2+\beta^2\lambda^2+\beta^2\right)\right]f_1=0 \tag{4.15}$$

$$D_5f_2-D_6f_1^2+D_7f_1^2f_2-4K_1f_0-3K_1f_2-4K_2\alpha^2f_2=0 \tag{4.16}$$

$$2f_0+f_2-\frac{1}{4}Rf_1^2\beta^2+2R\left(C_{26}^*\phi_1-C_{12}^*\phi_{1x}^T+C_{11}^*\phi_{1y}^T\right)=0 \tag{4.17}$$

From expression (4.15, 4.16, 4.17), lead to

$$\tau=-\frac{1}{2h\beta^2\lambda}\left\{D_1+D_2\frac{2D_6f_1^2+K_1Rf_1^2\beta^2-8K_1R\left(C_{26}^*\phi_1-C_{12}^*\phi_{1x}^T+C_{11}^*\phi_{1y}^T\right)}{2\left(D_5+D_7f_1^2-K_1-4K_2\alpha^2\right)}+D_3f_1^2\right.$$
$$\left.+D_4\left[\frac{2D_6f_1^2+K_1Rf_1^2\beta^2-8K_1R\left(C_{26}^*\phi_1-C_{12}^*\phi_{1x}^T+C_{11}^*\phi_{1y}^T\right)}{2\left(D_5+D_7f_1^2-K_1-4K_2\alpha^2\right)}\right]^2-K_1-K_2\left(\alpha^2+\beta^2\lambda^2+\beta^2\right)\right\} \tag{4.18}$$

That the maximal deflection of shells

$$W_{\max}=\frac{1}{8}Rf_1^2\beta^2-R\left(C_{26}^*\phi_1-C_{12}^*\phi_{1x}^T+C_{11}^*\phi_{1y}^T\right)+f_1$$
$$+\frac{2D_6f_1^2+K_1Rf_1^2\beta^2-8K_1R\left(C_{26}^*\phi_1-C_{12}^*\phi_{1x}^T+C_{11}^*\phi_{1y}^T\right)}{4\left(D_5+D_7f_1^2-K_1-4K_2\alpha^2\right)} \tag{4.24}$$

The twist angle of the shell is defined as

$$\psi=C_{33}^*\tau h+\frac{n^2\lambda}{4R^2}f_1^2 \tag{4.27}$$

By merging Eq. (4.18) and Eq. (4.42), it becomes possible to scrutinize

the impact of material and geometric factors on the post-buckling load-maximum deflection curves of shells.

The $\tau - \psi$ relation curve of shells can be derived by a combination of Eq. (4.18) and Eq. (4.27). From Eq. (4.27), it is clear that the relation between twist angle ψ and shear stress is linear when $f_1 = 0$. Furthermore, $\psi = 0$ when $f_1 = 0$ and $\tau = 0$, therefore the $\tau - \psi$ curve passes through the original coordinates.

Survey results

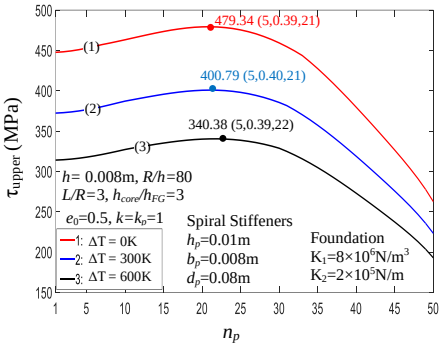

Figure 4.2a. Effects of ΔT on τ - n_p curves

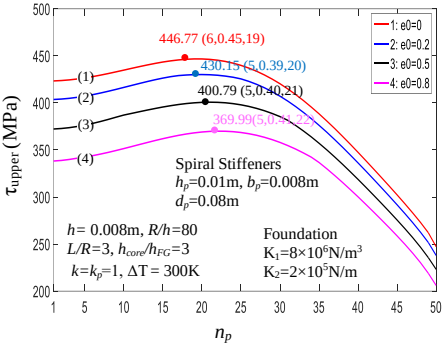

Figure 4.2b. Effects of e_0 on τ - n_p curves

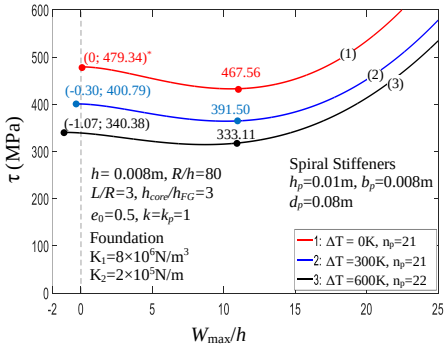

Figure 4.3a. Effects of ΔT on $\tau - W_{max}/h$ curves

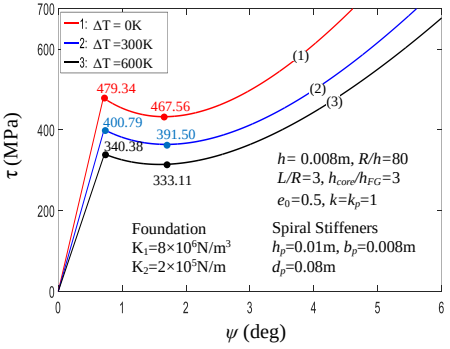

Figure 4.3b. Effects of ΔT on $\tau - \psi$ curves

Figs. 4.2a and 4.2b show that each different set of parameters will give different optimal n_p values. This indicates that increasing the number of stiffeners does not always increase the bearing capacity of the cylindrical

shell. Since the number of stiffeners depends on the angle of stiffeners, when the number of stiffeners changes, the angle of the stiffeners also changes, resulting in a change in the bearing capacity.

In addtion, Fig. 2b illustrates the effect of the porosity coefficient on the upper critical loads. Obviously, an increase in the pososity coefficient e_0 reduces the stiffness of FGP cylindrical shells, resulting in a decrease in the upper critical loads.

Combining Eq. (4.18) and Eqs. (4.24), (4.27), Figs. 3a and 3b are presented. They describe the effect of temperature on the $\tau - W_{max}/h$ and $\tau - \psi$ curves. In Fig. 3a, curves 2 and 3 do not start at a point on the y-axis of coordinates. That means the temperature field causes the shell to deflect outward (negative deflection) before it is subjected to mechanical load. When the shell is under torsional load, its outward deflection decreases until the torsional load reaches the bifurcation point, an inward deflection occurs.

4.3. Nonlinear stability of ES-FG porous sandwich cylindrical shells subjected to torsional load

Consider an eccentrically stiffened FG-porous cylinder subjected to external pressure as shown in figure 3.7.

The nonlinear equilibrium equations of cylindrical shell, taking into account an elastic foundation, based on the first order shear deformation theory are given by Eqs. (4.37-4.41)

Assume that a torsion-loaded cylindrical shell surrounded by elastic foundations in thermal environment and it is simply supported at two butt-ends $x = 0$ and $x = L$. In this case, the deflection of shell is expressed by

$$\begin{aligned} &u = U\sin\left(\frac{m\pi x}{L} + \frac{ny}{R}\right);\ \mathrm{v} = V\sin\left(\frac{m\pi x}{L} + \frac{ny}{R}\right);\ w = W\cos\left(\frac{m\pi x}{L} + \frac{ny}{R}\right) \\ &\phi_x = \Phi_x\sin\left(\frac{m\pi x}{L} + \frac{ny}{R}\right);\ \phi_y = \Phi_y\sin\left(\frac{m\pi x}{L} + \frac{ny}{R}\right) \end{aligned} \tag{4.42}$$

Introduction of Eq. (4.42) into Eqs. (4.37-4.41), then applying Galerkin method in the ranges $0 \le y \le 2\pi R$ and $0 \le x \le L$, lead to

$$\tau = -\frac{LR}{2mn\pi h}\left[\begin{aligned} &a_{31}\frac{D_1}{D} + a_{32}\frac{D_2}{D} + a_{33} + \left(\phi_1 + \phi_{1x}^T\right)\frac{m^2\pi^2}{L^2} + \left(\phi_1 + \phi_{1y}^T\right)\frac{n^2}{R^2} \\ &-K_1 - K_2\left(\frac{m^2\pi^2}{L^2} + \frac{n^2}{R^2}\right) + a_{34}\frac{D_3}{D} + a_{35}\frac{D_4}{D} + a_{36}W^2 \end{aligned}\right] \tag{4.49}$$

Based on Eq. (4.49), the nonlinear buckling and post-buckling of ES-FGM cylindrical shell surrounded by elastic foundations and in thermal environment are analyzed.

Survey results

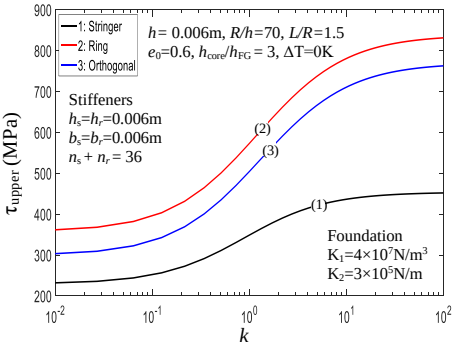

Figure 4.20. Effects of stiffeners and k on upper torsional load τ_{upper}

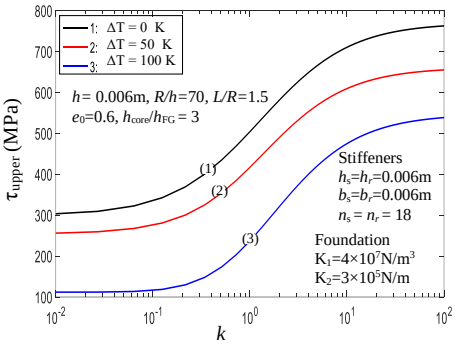

Figure 4.21. Effects of stiffeners and k on upper torsional load τ_{upper}

The effects of volume fraction index on the critical buckling load of FGP shell are considered in 10 and 11. It is found that, the critical buckling load decreases with the increase of k. This property is suitable to the real property of material, because the higher value of k corresponds to a metal-richer shell which usually has less stiffness than a ceramic-richer one.

The effects of stiffeners on critical loads are given in Figs. 10. As can be seen that, the critical load of FGP shell reinforced by stringers is the smallest, the critical load of FGP cylindrical shell reinforced by rings is biggest.

The effects of temperature on buckling load are also shown in Fig. 11. It can be seen that the upper torsional load of shell reduces when ΔT increases.

Conclusion of Chapter 4

The content of Chapter 4 of the thesis addresses the following issues

1. Analyzed nonlinear behavior of FG porous cylindrical sandwich shells reinforced by spiral stiffeners under torsional load.

2. Analyzed nonlinear stability of ES-FG porous sandwich cylindrical shells subjected to torsional load.

CONCLUDE

The thesis has the following outstanding new contributions

1. The thesis has established analytical expressions for the influence of 4 porosity distribution models on the nonlinear stability of FGP cylindrical plate structures and FGP cylindrical shells subjected to axial compression.

2. The thesis uses Donnell shell theory, the thesis has established nonlinear stability analysis expressions of FGP sandwich cylindrical panels subjected to axial compression. Then, use the Galerkin method to find the ultimate load and draw the load-deflection curve describing the post-critical response of the structure.

3. The thesis uses Donnell shell theory, the first order shear deformation theory, the improved Lekhnitskii's smeared stiffeners technique, Galerkin method is applied to find the ultimate load and draw the load-deflection curve describing the post-critical response of cylindrical sandwich FGP subjected to mechanical loads in thermal environment.

4. Numerical investigation, analyzing the influence of input parameters such as: types of void distribution, pore density coefficient, volume fraction, imperfection, boundary conditions, geometrical dimensions, ribs, foundation, heat, to the problem of nonlinear stability of FGP cylindrical panels and FGP cylindrical shells.

5. In the chapters, the thesis has drawn a number of comments that have scientific and practical value for designers and manufacturers of shell structures made of FGP materials.

LIST OF PUBLISHED WORKS RELATED TO THE THESIS

1. Do Quang Chan, **Pham Van Hoan**, Nguyen Thoi Trung, Le Kha Hoa, Duong Thanh Huan, 2021, Nonlinear buckling and post-buckling of imperfect FG porous sandwich cylindrical panels subjected to axial loading under various boundary conditions, *Acta Mechanica*, 232, pp. 1163-1179. (ISI, Q2).

2. **Phạm Văn Hoàn**, Đào Như Mai và Lê Khả Hòa, 2021, Phân tích ảnh hưởng mô hình phân bố độ xốp đến sự ổn định của panel trụ làm bằng vật liệu FGP, *Hội nghị Khoa học toàn quốc Cơ học Vật rắn lần thứ XV Trường Đại học Kỹ thuật Công nghiệp, Đại học Thái Nguyên TP. Thái Nguyên, ngày 24, 25 tháng 9 năm 2021*, pp. 412-421.

3. **Pham Van Hoan**, Dao Nhu Mai, Khuc Van Phu, Le Kha Hoa, 2022, Nonlinear buckling and post-buckling of imperfect FG porous sandwich cylindrical panels subjected to axial loading on elastic foundation, *Vietnam Journal of Mechanics*, 44(4), pp. 514-525.

4. Le Kha Hoa, **Pham Van Hoan**, Bui Thi Thu Hoai & Do Quang Chan, 2021, Nonlinear Buckling and Postbuckling of ES-FG Porous Cylindrical Shells Under External Pressure, *Modern Mechanics and Applications*, pp. 743-754. (Scopus Q4).

5. Le Kha Hoa, **Pham Van Hoan**, and Dao Nhu Mai, 2022, Influence of porosity distribution pattern on the nonlinear stability of porous cylindrical shells under axial compression, *Tuyển tập công trình khoa học Hội nghị Cơ học toàn quốc lần thứ XI. Tập 1, Cơ học vật rắn biến dạng. Hà Nội, 02-03/12/2022*, pp. 380-390.

6. **Pham Van Hoan**, Le Kha Hoa, 2024, Nonlinear stability of ES-FG porous sandwich cylindrical shells subjected to axial compression in thermal environment, *Structures*, 63, 106280. (ISI, Q1).

7. **Phạm Văn Hoàn**, Đào Như Mai, Khúc Văn Phú và Lê Khả Hòa, 2024, Ổn định phi tuyến của vỏ trụ sandwich FGP có gân FGM gia cường chịu nén dọc trục, *Hội nghị Cơ học toàn quốc Kỷ niệm 45 năm thành lập Viện Cơ học 09/4/2024*, pp. 256-265.

8. Tran Minh Tu, Duc-Kien Thai, **Pham Van Hoan** &Le Kha Hoa, 2022, *Nonlinear behavior of FG porous cylindrical sandwich shells reinforced by spiral stiffeners under torsional load including thermal effect*, Mechanics of Advanced Materials and Structures, 29(27), pp. 5860-5875. (ISI, Q2).

9. **Pham Van Hoan**, Dao Nhu Mai, Phan Van Ba and Le Kha Hoa, 2024, Analyzing the nonlinear torsional buckling and post-buckling of ES - FG Porous cylindrical shells in thermal environment using FSDT in terms of the displacement components, *Vietnam Journal of Mechanics*, 46(1), pp. 67-79.